

Nonlinear Compressional Pulses in a 2D Crystallized Dusty Plasma

V. Nosenko,* S. Nunomura,† and J. Goree‡

Department of Physics and Astronomy, The University of Iowa, Iowa City, Iowa 52242

(Received 6 March 2002; published 8 May 2002)

Compressional pulses were launched in a two-dimensional Yukawa lattice, a hexagonal monolayer of polymer microspheres suspended in a plasma. The pulsed wave was excited by a laser beam, and nonlinear effects were observed for Mach numbers $M > 0.07$ and for variation of particle number density $\delta n/n > 0.1$, but no steepening of the pulse was detected. The pulse propagation speed was found to be comparable to the sound speed of compressional waves launched with sinusoidal excitation.

DOI: 10.1103/PhysRevLett.88.215002

PACS numbers: 52.27.Lw, 52.27.Gr, 52.35.Mw, 82.70.Dd

Two-dimensional ordered lattices are found in a variety of physical systems, including dusty plasmas [1–4] and colloidal suspensions [5], where particles interact through a screened Coulomb repulsion or Yukawa potential. Such a lattice can have either a crystalline or a liquidlike order. It sustains compressional waves and, in a crystalline or highly ordered liquid phase, transverse shear waves [5–12].

Here we report experiments with pulsed compressional waves in a 2D plasma crystal. The term “plasma crystal” refers to a suspension of small particles of solid matter, which are immersed in a plasma containing free electrons, ions, and neutral gas. The particles acquire a negative charge Q , and in the presence of gravity they are levitated by the electric field in the sheath above a horizontal lower electrode. In the radial direction, particles are trapped by weaker radial fields in the plasma. Experiments by Konopka *et al.* [13] have shown that in the horizontal direction the interparticle force is modeled accurately by a Yukawa potential $U(r) = Q(4\pi\epsilon_0 r)^{-1} \exp(-r/\lambda_D)$, where λ_D is the Debye length. When many such particles are trapped in a horizontal monolayer, they arrange in a triangular lattice with hexagonal symmetry. The lattice is characterized by a screening parameter $\kappa = a/\lambda_D$, where a is the interparticle spacing.

A two-dimensional lattice with Yukawa interparticle potential can be modeled as a network of masses connected by springs to the nearest neighbors, and by weaker springs to more distant particles. If the particle displacement is small, the spring will be linear, with a restoring force proportional to displacement [14]. Nonlinear effects arise when the spring is compressed or extended by large amplitude.

Linear sound waves in a two-dimensional screened-Coulomb lattice have dispersion relations that have been derived theoretically [5–10] and verified experimentally [11,12]. For short wavelengths, they exhibit dispersion, i.e., frequency ω is not proportional to wave number k . On the other hand, for long wavelengths, the propagation of linear compressional sound waves is dispersionless, with a speed $\omega/k = C_L$ given by [8]

$$C_L = Qa(4\pi\epsilon_0 ma^3)^{-1/2}(4\pi/\sqrt{3})^{1/2}\kappa^{-1/2}, \quad (1)$$

where m is the particle mass. Note that C_L does not depend on the wave amplitude. These theories are for linear waves with small amplitude.

The nonlinear behavior of the waves at large amplitude has not been studied as completely as the linear behavior. Theoretically, the possibility that the compressional waves can propagate in a nonlinear regime as solitary waves was demonstrated for 3D weakly coupled [15] and 2D strongly coupled [16] dusty plasmas. Experimentally, nonlinear waves in dusty plasmas were possibly observed in the laser-excited compressional Mach-cone experiments of Melzer *et al.* [17], although the size of error bars did not allow the authors to conclude this definitely. Here we report an experiment intended to observe nonlinear effects using a laser that is 3 times more powerful than in Ref. [17], and by launching compressional waves in the form of pulses instead of Mach cones. Laser excitation provides a purely local initial perturbation, without disturbing the horizontal forces that trap particles. In another approach, an electrical wire launches pulses [16], but additional long-range attractive and repulsive forces act in the horizontal direction on the plasma crystal [18].

In our apparatus, Fig. 1, a plasma was produced using a capacitively coupled parallel-plate rf discharge. To reduce the damping rate, we used Ar at a low pressure of 15 mTorr, so that the Epstein drag was only $\nu = 2.9 \text{ s}^{-1}$ [19]. The plasma was sustained by a 13.56 MHz rf voltage with a peak-to-peak amplitude of 138 V and a self-bias of -90 V . Langmuir probe measurements at a point in the bulk plasma, well above the sheath region, indicated an electron temperature $T_e = 2.5 \text{ eV}$, plasma potential $V_p = 21 \text{ V}$, and ion density $n_i = 3.5 \times 10^{15} \text{ m}^{-3}$.

Our polymer microspheres formed a hexagonal lattice with a diameter of about 60 μm . Depending on the number of particles that we introduced, a ranged from 486 μm to 1097 μm . The microspheres had a diameter of $8.09 \pm 0.18 \mu\text{m}$ measured using TEM and a mass density 1.514 g/cm^3 . The particle charge was measured to be $Q = -9000 \pm 200e$, and the Debye screening length was

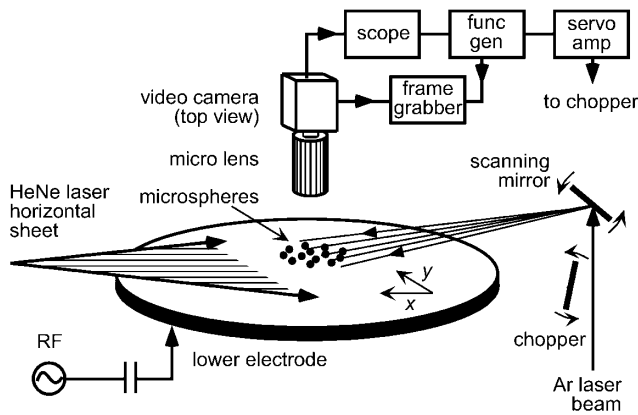


FIG. 1. Experimental apparatus. Polymer microspheres levitate above the lower electrode in a capacitively coupled parallel-plate rf plasma. The particles settle in a single horizontal layer, arranged in a hexagonal lattice. Compressional pulses are excited in the lattice by applying a modulated laser sheet.

measured to be $\lambda_D = 0.73 \pm 0.10$ mm at the particles' height, using a wave technique [12]. The pair correlation function $g(r)$ of the lattice had many peaks, and its translational order length was 4 to 20 interparticle spacings; this indicates that the lattice was in an ordered state.

Our primary measurements were the particle velocities and areal number densities, which we computed from the particle positions. The latter were recorded for 64 consecutive frames in a 30 frame-per-second digital movie, based on a video recording using a top-view camera. The camera imaged particles illuminated by a horizontal sheet of HeNe laser light, and its field of view was 24×18 mm, which included 400–2000 particles. The particle positions were calculated with subpixel resolution using the moment method [17].

We used the laser-manipulation method of Homann *et al.* [14,20] to excite compressional pulses in the plasma crystal. Particles were accelerated at a rate proportional to the incident laser intensity [21]. An Ar laser intensity was modulated with a scanning mirror that chopped the laser beam on and off, while another scanning mirror that oscillated rapidly at 200 Hz was used to expand the laser beam into a sheet, which struck the lattice at an angle of 10° with respect to the horizontal lattice plane. The laser power was 0.66–2.75 W, which we measured just before the vacuum chamber window. At its focus in the vacuum chamber, the laser beam had a Gaussian profile with a full width at half maximum of 0.6 mm, at our lowest power of 0.66 W. The excitation pulse wave form was trapezoidal; the rise time was 10% of the pulse duration, and so was the decay time. The k spectrum corresponding to our laser beam shape had 12% and $<1\%$ of its power for ka above 0.6 and 1.6, respectively, for $a = 0.8$ mm. These values of ka mark the onset of dispersion and its dependence on the lattice orientation, respectively, according to the theoretical dispersion relation [7].

The video was synchronized to the excitation pulses using the triggering scheme described in Ref. [17], with one laser pulse in each frame. This allowed us to average the data for ten laser excitation pulses, all under the same conditions, to improve the signal-to-noise ratio. The excitation pulses were repeated at an interval of 2.4 s.

Each laser pulse excited a pulse of compressional waves in the lattice, which we measured using our time-resolved maps of the particle velocity and areal number density. To analyze the pulse propagation, we divided the maps into 50 rectangular bins, which were elongated along the y axis. In each bin, the v_x component of the particle velocity was averaged, while the v_y component was ignored, because it was much smaller. In this way, we prepared Fig. 2, showing the particle velocity profiles in the direction of pulse propagation x .

The pulse propagation speed C was measured by determining the position x_0 of the peak in each frame, and then fitting x_0 vs t to a straight line. The peak's position x_0 was measured in a two-step process. As a first estimate of x_0 , we identified the point x_{\max} , where v_x had its maximum. Then, to reduce the effect of noise, we calculated the first moment of v_x vs x using data in a range of x from $x_{\max} - 2.5$ mm to $x_{\max} + 2.5$ mm. We found C in the range 9–26.5 mm/s, depending on the interparticle spacing. We found that the pulse propagation speed increases with particle number density (decreases with screening parameter κ), in agreement with Eq. (1). The pulse was damped, as it propagated away from the excitation region, with a scale length of ≈ 10 mm, as expected based on Epstein drag and the value of C .

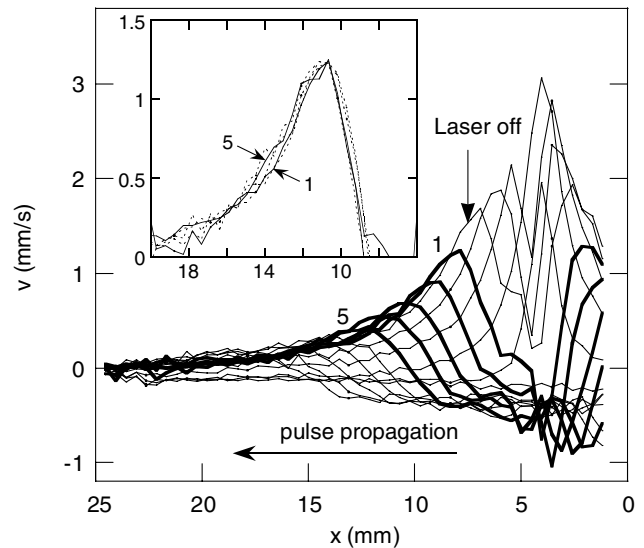


FIG. 2. Propagation of a compressional pulse. Particle velocity profiles are shown in the direction of the pulse propagation, for screening parameter $\kappa = 1.45$ and a laser power of 2.38 W. The curves are separated by 0.1 s. The bold curves are after the laser is off; these curves were used to measure the pulse propagation speed. In the inset, the curves are shown shifted and rescaled, so that their maxima coincide.

We performed three different tests intended to observe nonlinearity in the pulse propagation. First, we measured the pulse propagation speed vs excitation laser power. Second, we compared the pulse amplitudes measured in terms of velocity and number density. Third, we evaluated the pulse shape, looking for its possible steepening. In all three tests, the pulse duration was a constant $\tau = 0.5$ s, to isolate the effects of nonlinearity from those of dispersion.

Our first test of nonlinearity, a measurement of the pulse propagation speed for different values of excitation laser power, provides evidence of nonlinearity. The results are shown in Fig. 3. If the pulse were linear, its speed would obey Eq. (1), independent of the amplitude. Instead, we observed a faster propagation speed at higher excitation power. This indication of nonlinearity is present at larger values of κ , but not at smaller values of κ , apparently due to our limited laser power.

It is a common characteristic of nonlinear waves that the speed of wave propagation C depends on the wave amplitude in velocity space v . Although we do not have an analytic theory of this dependence for our 2D Yukawa crystal, it is instructive to consider the following expression for the different case of an adiabatic sound wave in an ideal fluid [22]:

$$C = C_L + 0.5(\gamma - 1)v. \quad (2)$$

Here, γ is the adiabatic coefficient.

In Fig. 3, both the pulse propagation speed and the pulse amplitude are normalized by the speed of pulse propagation at a low amplitude corresponding to our lowest excitation laser power of 0.66 W. This allows us to present the data for all values of κ together, showing the dependence

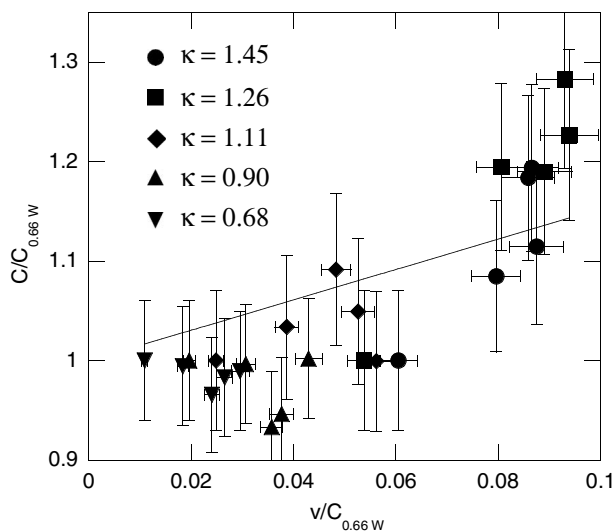


FIG. 3. Dependence of the pulse propagation speed C on the pulse amplitude in velocity space v . Both axes are normalized by the pulse propagation speed $C_{0.66 \text{ W}}$ for the lowest laser power we used, 0.66 W. Nonlinear effects are revealed by the speed of the pulse increasing with its amplitude; this trend is indicated empirically by the straight line, which is a fit to all the data.

on amplitude. The pulse propagation speed has a general upward trend with pulse amplitude, in agreement with Eq. (2). Perhaps our data in Fig. 3 should be fitted to some shape other than a straight line as suggested by Eq. (2), because our experimental system is a 2D hexagonal lattice where the sound speed is independent of temperature, whereas Eq. (2) was originally derived for an adiabatic motion in an ideal fluid, where the sound speed depends on the temperature.

Our second test of nonlinearity, the dependence of the particle speed v vs variation of particle number density $\delta n/n$, also revealed nonlinear effects. In this test, we compared the pulse amplitude measured in velocity space with the pulse amplitude measured in number density space. For this purpose, we define the amplitudes of v and $\delta n/n$ as their peak value for profile at a given time. In theory, linear waves with no dispersion are characterized by

$$v/C_L = \delta n/n. \quad (3)$$

Our results in Fig. 4 deviate from Eq. (3), indicating nonlinear motion. This deviation is apparent when $\delta n/n > 0.1$, for higher values of κ and higher laser power. The effect is biggest in the excitation region, because the amplitudes are largest there. The straight line in Fig. 4 corresponds to the sound speed C_L of linear waves, using Eq. (3). Note that Eq. (3) is based on conservation of the particle number, which was satisfied in our experiment and analysis.

As the third test of nonlinearity, we evaluated the pulse's shape, as it propagated through the lattice. In the inset of

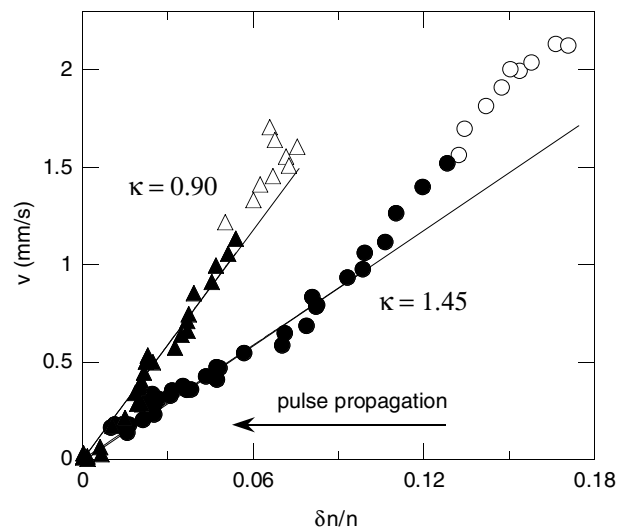


FIG. 4. Pulse amplitude in velocity space v vs pulse amplitude in number density space $\delta n/n$. Both amplitudes decrease as the pulse propagates through the lattice. Shown are data for two values of the screening parameter $\kappa = 1.45$ (circles) and $\kappa = 0.90$ (triangles). The excitation laser power was 2.38 W. Solid symbols represent data recorded outside of the excitation region, and open symbols inside it. Deviation from the linear dependence of Eq. (3) is an indication of nonlinearity.

Fig. 2, we shifted the velocity profiles of the propagating pulse at different times so that their maxima coincided, and we rescaled the vertical axis to eliminate the effect of damping as the pulse propagated through the lattice.

Unlike the first two tests, the third test did not show any nonlinear effects that we could identify. The pulse's shape showed no significant change as pulse propagated through the crystal. In particular, we observed no visible steepening of the wave front, as would be expected in shock formation, for example. Perhaps steepening of the pulse is a less sensitive test of nonlinearity than the other two tests. Or, perhaps this method requires that nonlinear effects accumulate over a distance that is a much greater multiple of the pulse width than in our experiment. The pulse shapes shown in the inset of Fig. 2 actually broadened, rather than steepened, as they propagated away from the excitation region; this might be an indication of dispersion.

To test the role of dispersion in the pulse propagation, another experiment was carried out, using different durations of excitation pulse, $\tau = 0.05\text{--}0.2$ s. To isolate the effects of dispersion from those of nonlinearity, the pulse energy, i.e., the product of excitation laser power and the pulse duration, was kept constant at 0.14 J. We expected shorter pulses to have more spectral content at high frequencies. For the entire range of τ that we tested, we note that $2\pi/\tau > 1.5\omega_0$, where ω_0 is a 2D analog of plasma frequency, $\omega_0^2 = Q^2/4\pi\epsilon_0 m a^3$, and m is the particle mass. Compressional waves in a 2D lattice show deviation from acoustic dispersion for frequencies $\omega > 1.3\omega_0$ [7]. Therefore, one might expect to detect dispersion in this test. However, we found no obvious dependence of the pulse propagation speed on the duration of excitation pulse, and, hence, on the pulse's frequency spectrum. This means that, given the size of error bars, dispersion is not detectable using this method at these experimental conditions. This might be due to the limitation posed by the k spectrum corresponding to the laser-beam's spatial profile, which had only 1%–26% (depending on a) of its energy at wave numbers $ka > 0.6$, corresponding to $\omega > 1.3\omega_0$.

In conclusion, we can say that we observed nonlinear effects in the pulse propagation, but for the laser excitation levels we used these nonlinear effects were weak. Increasing the laser power from 0.66 to 2.75 W gave rise to an increase in the pulse propagation speed of up to 22%, in the case of $\kappa = 1.26$. In our experiment, we achieved pulse amplitudes of $v/C_L < 0.1$ in Fig. 3 and $\delta n/n < 0.13$ in Fig. 4, while in the excitation region the

highest Mach number for particle speed we achieved was $v/C_L = 0.39$ and the maximum variation of number density was $\delta n/n = 0.22$. This latter value is comparable to the highest level achieved in the laser-excited Mach cone experiment of Melzer *et al.*, and half that in the wire-excited pulse experiment of Samsonov *et al.* [16].

We thank K. Avinash, R. Merlino, A. Piel, F. Skiff, and V. Steinberg for valuable discussions and L. Boufendi for TEM measurements. This work was supported by NASA, NSF, and DOE. S.N. was supported by the Japan Society for the Promotion of Science.

*Electronic mail:

†Present address: Max-Planck-Institut für Extraterrestrische Physik, D-85740 Garching, Germany.

‡Electronic mail:

- [1] J. H. Chu and Lin I, Phys. Rev. Lett. **72**, 4009 (1994).
- [2] H. Thomas *et al.*, Phys. Rev. Lett. **73**, 652 (1994).
- [3] Y. Hayashi and K. Tachibana, Jpn. J. Appl. Phys. **33**, L804 (1994).
- [4] A. Melzer, T. Trottenberg, and A. Piel, Phys. Lett. A **191**, 301 (1994).
- [5] F. M. Peeters and X. Wu, Phys. Rev. A **35**, 3109 (1987).
- [6] R. S. Crandall, Phys. Rev. A **8**, 2136 (1973).
- [7] D. H. E. Dubin, Phys. Plasmas **7**, 3895 (2000).
- [8] X. Wang, A. Bhattacharjee, and S. Hu, Phys. Rev. Lett. **86**, 2569 (2001).
- [9] P. K. Kaw and A. Sen, Phys. Plasmas **5**, 3552 (1998).
- [10] G. Kalman, M. Rosenberg, and H. E. DeWitt, Phys. Rev. Lett. **84**, 6030 (2000).
- [11] S. Nunomura, D. Samsonov, and J. Goree, Phys. Rev. Lett. **84**, 5141 (2000).
- [12] S. Nunomura, J. Goree, S. Hu, X. Wang, and A. Bhattacharjee, Phys. Rev. E (to be published).
- [13] U. Konopka, G. E. Morfill, and L. Ratke, Phys. Rev. Lett. **84**, 891 (2000).
- [14] A. Homann *et al.*, Phys. Lett. A **242**, 173 (1998).
- [15] N. N. Rao, P. K. Shukla, and M. Y. Yu, Planet. Space Sci. **38**, 543 (1990).
- [16] D. Samsonov *et al.*, Phys. Rev. Lett. **88**, 095004 (2002).
- [17] A. Melzer *et al.*, Phys. Rev. E **62**, 4162 (2000).
- [18] D. Samsonov *et al.*, Phys. Rev. E **63**, 025401(R) (2001).
- [19] P. Epstein, Phys. Rev. **23**, 710 (1924).
- [20] A. Homann *et al.*, Phys. Rev. E **56**, 7138 (1997).
- [21] A. Ashkin, Phys. Rev. Lett. **24**, 156 (1970).
- [22] L. D. Landau and E. M. Lifshitz, *Fluid Mechanics* (Butterworth-Heinemann, Boston, 1997), Vol. 6.